Quantized conductance

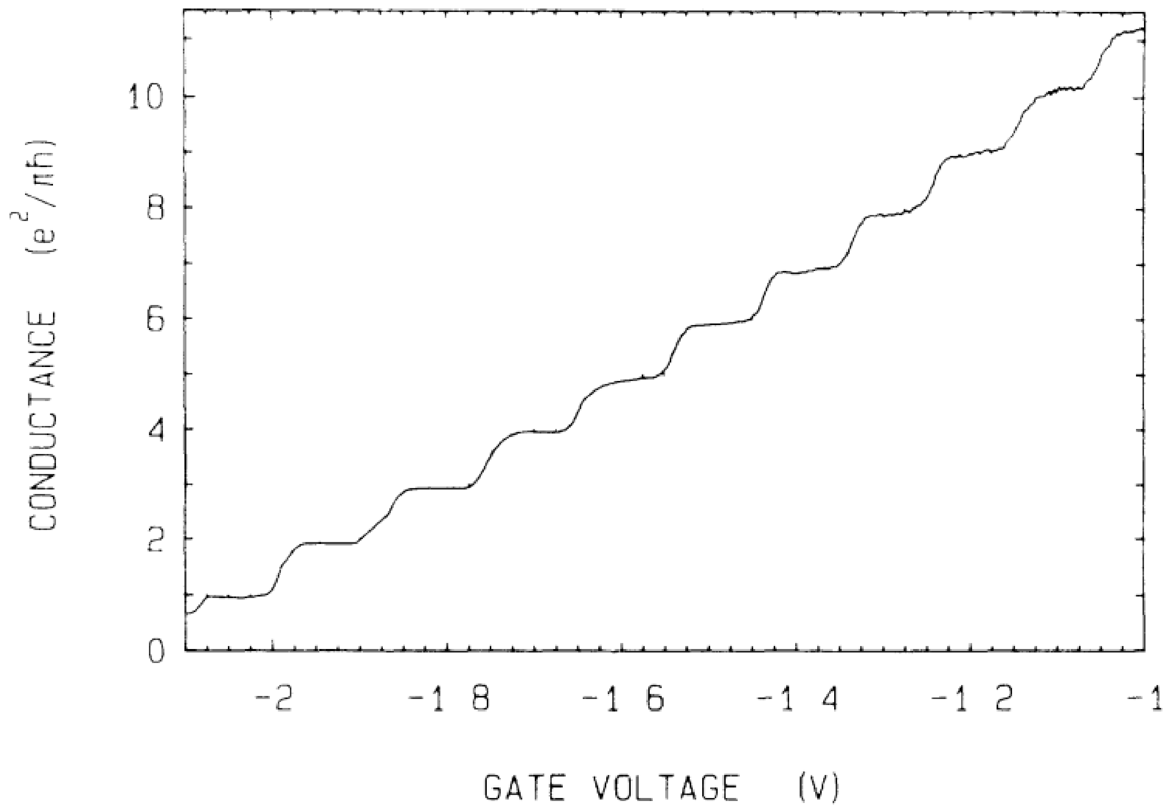

FIG. 2. Point-contact conductance as a function of gate voltage, obtained from the data of Fig. 1 after subtraction of the lead resistance. The conductance shows plateaus at multiples of $e^2/\pi\hbar$.

Phys. Rev. Lett. 60, 848 (1988)

Quantized conductance

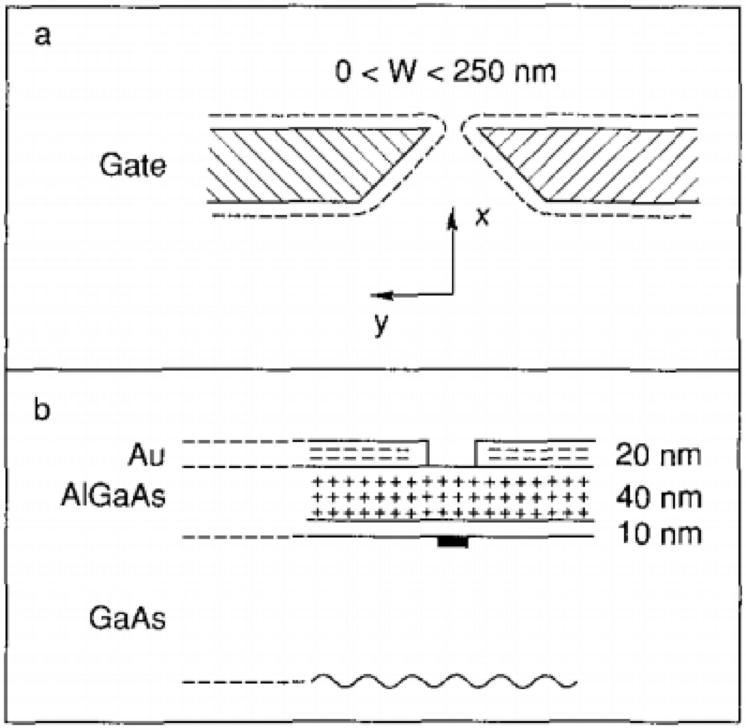

FIG 1 (*a*) Top view of a quantum point contact, defined using a split gate (shaded) on top of a GaAs-$Al_xGa_{1-x}As$ heterostructure The depletion boundary is indicated by the dashed curve The width W of the constriction can be reduced by increasing the negative voltage on the gate (*b*) Cross section of the quantum point contact The narrow quasi-one-dimensional electron gas channel in the constriction is indicated in black The positive ionized donors (+) in the AlGaAs layer are indicated, as well as the negative charge (−) on the gate

Phys. Rev. Lett. 60, 848 (1988)

Spin valves and tunneling junctions

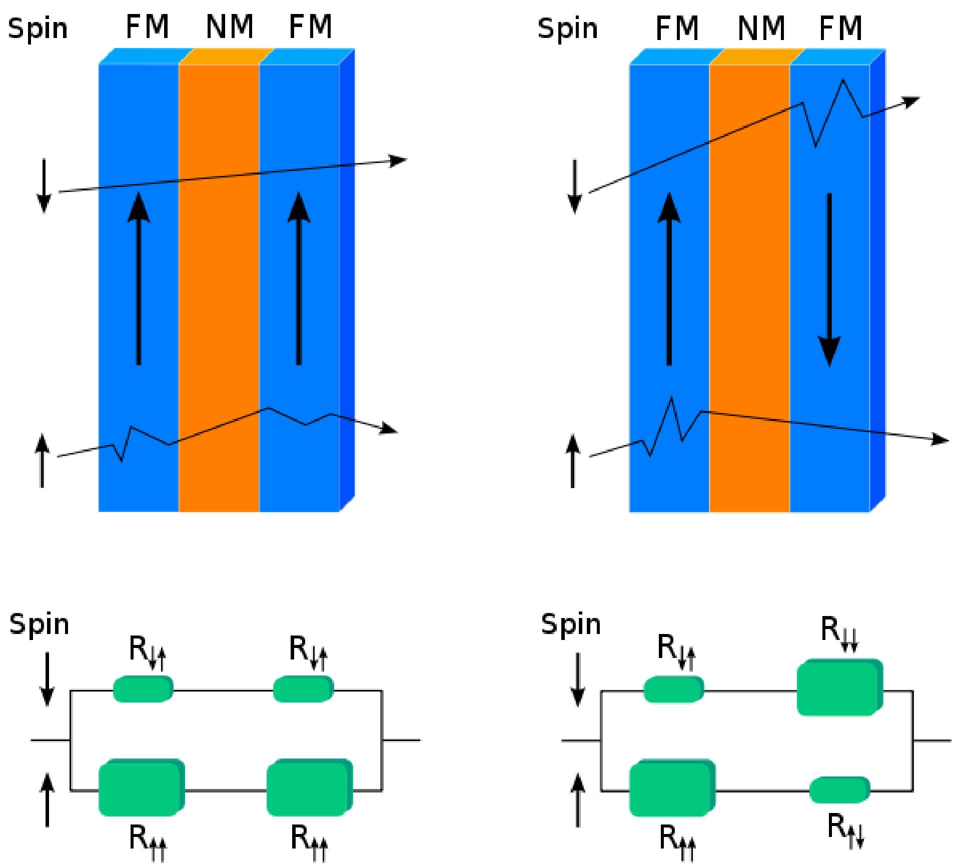

Spacer can be metal or an insulator

Giant Magnetoresistance – 2007 Nobel prize

Tunneling

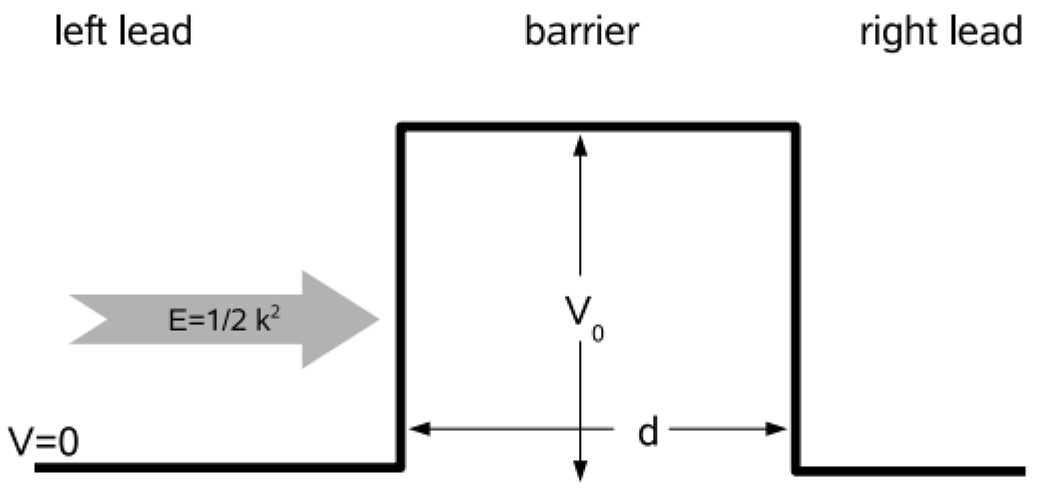

$$t \sim \frac{4i\kappa k\, e^{-ikd}}{(k+i\kappa)^2} e^{-\kappa d}.$$

Exponential decay

https://juser.fz-juelich.de/record/136125/files/Schluesseltech_10.pdf

Tunneling in MgO

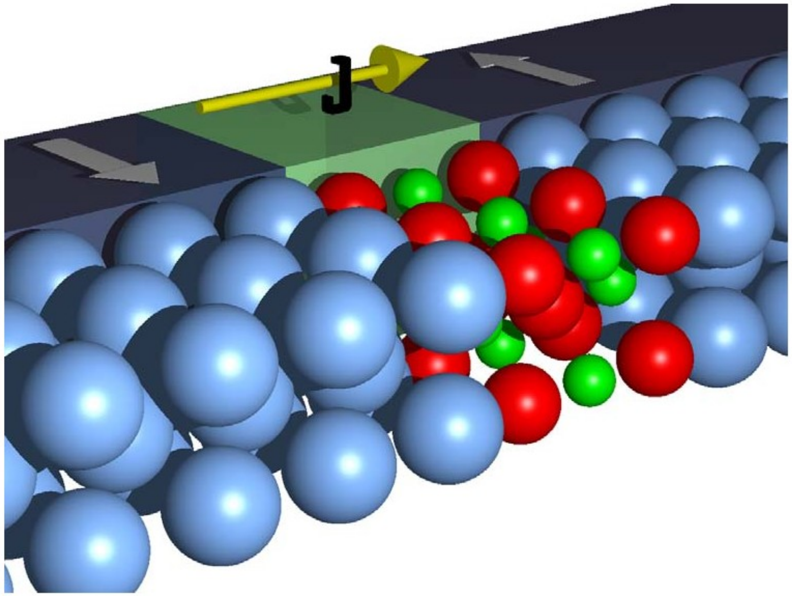

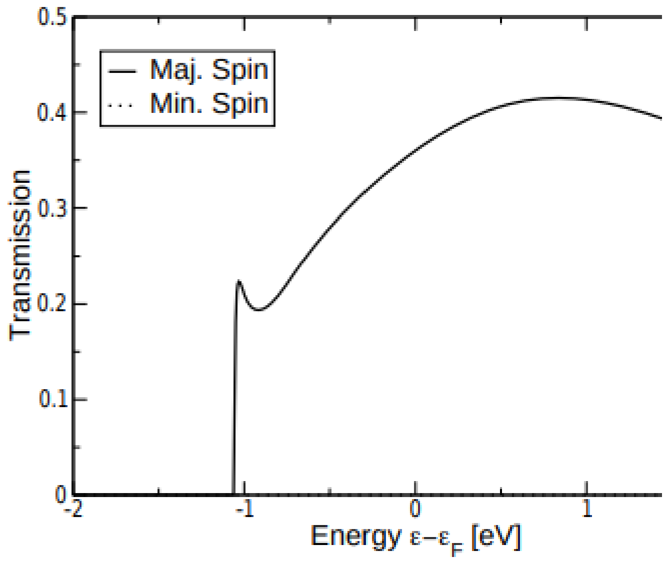

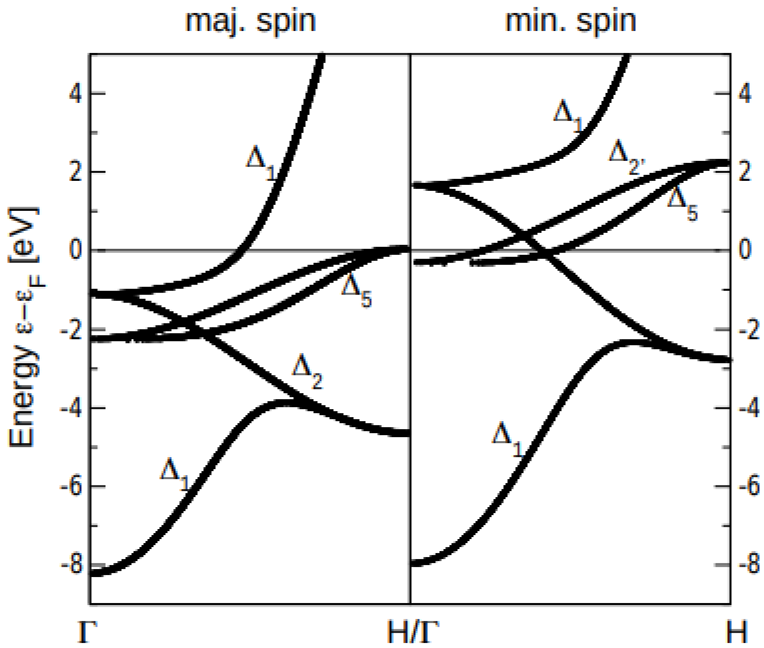

Periodic in the transverse directions

Channels are labeled by n,k_x and k_y

Tunneling in MgO

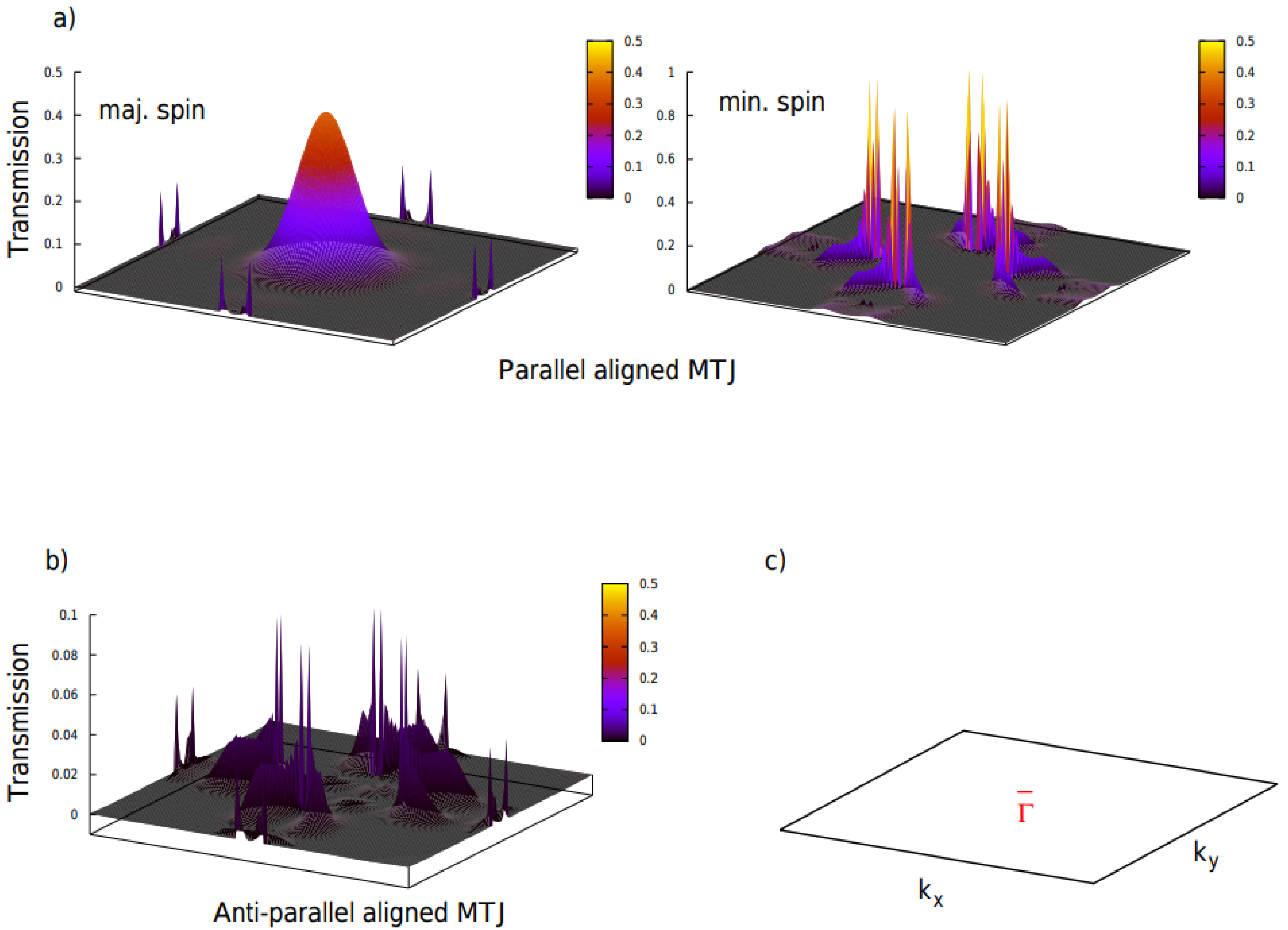

Calculated TMR can be 1000s of %, experimentally around 200%

Spin transfer torque

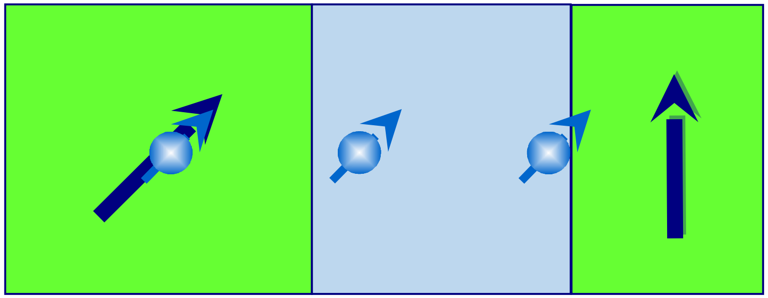

Berger PRB '96, Slonczewski JMMM '96

Transfer of spin from one layer to the other

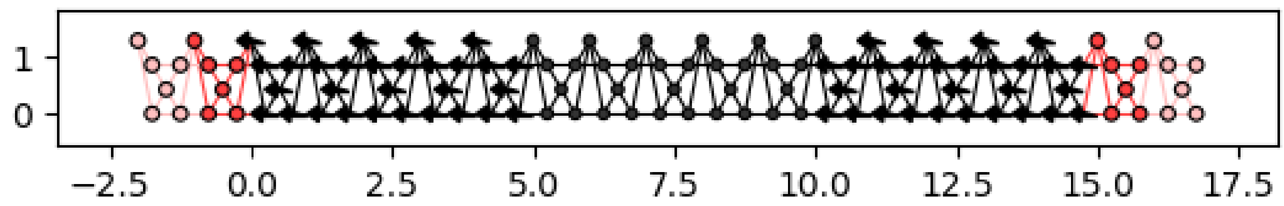

System periodic along y

Semi-infinite ferromagnetic layers

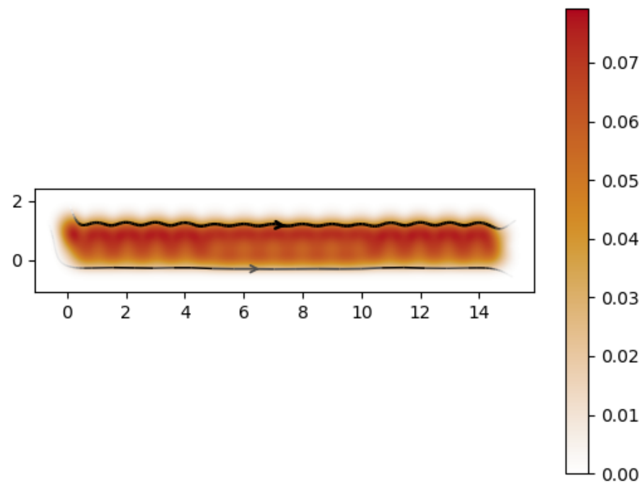

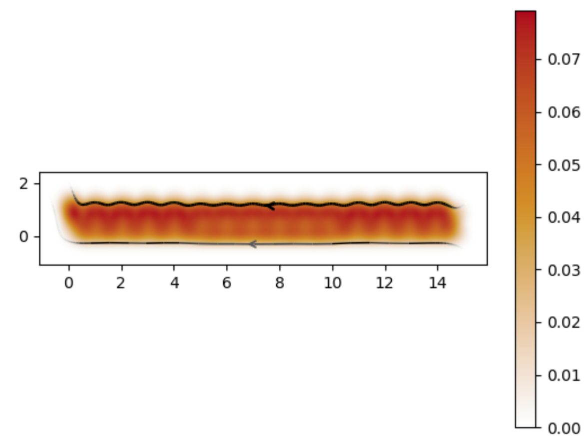

Charge current

spin current

Fully spin-polarized current

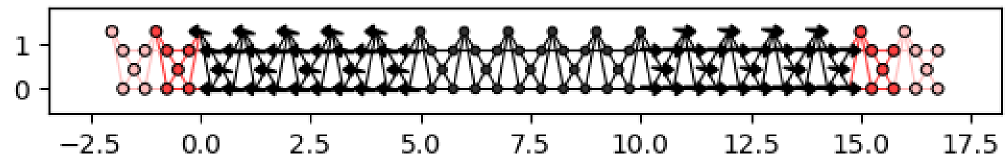

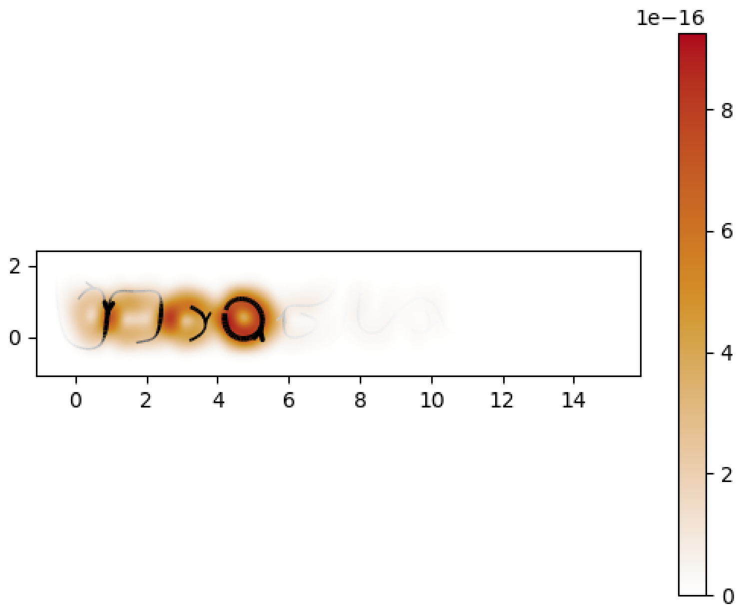

Charge current

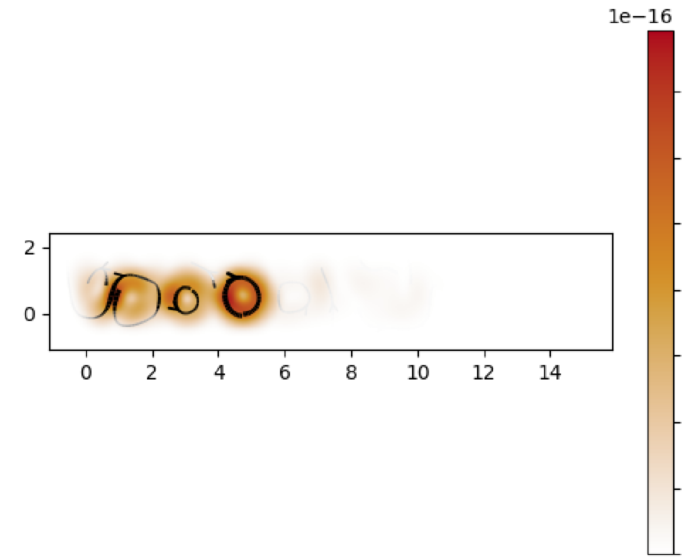

spin current

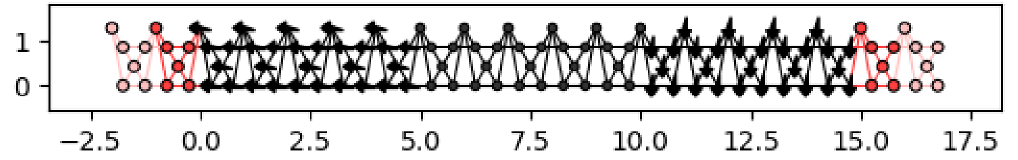

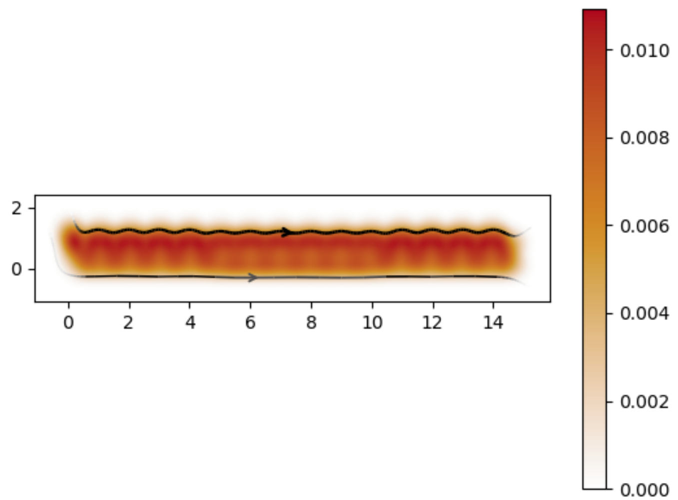

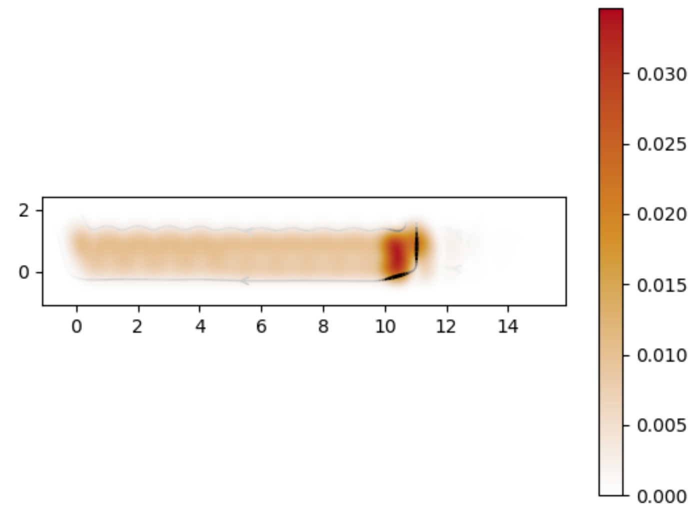

Charge current

spin current – x component

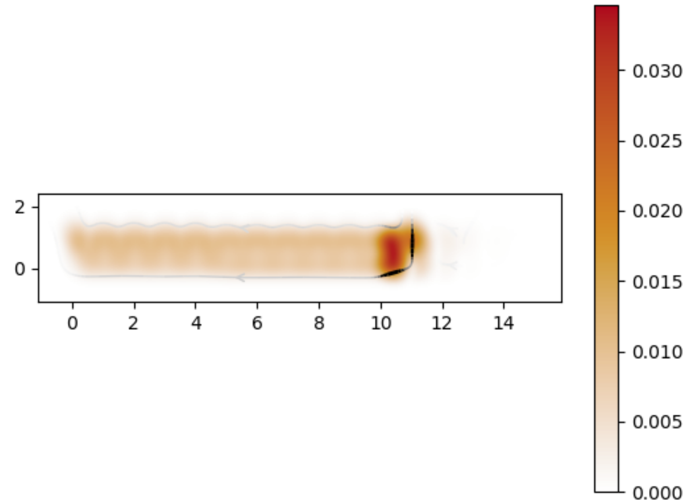

spin current – x component

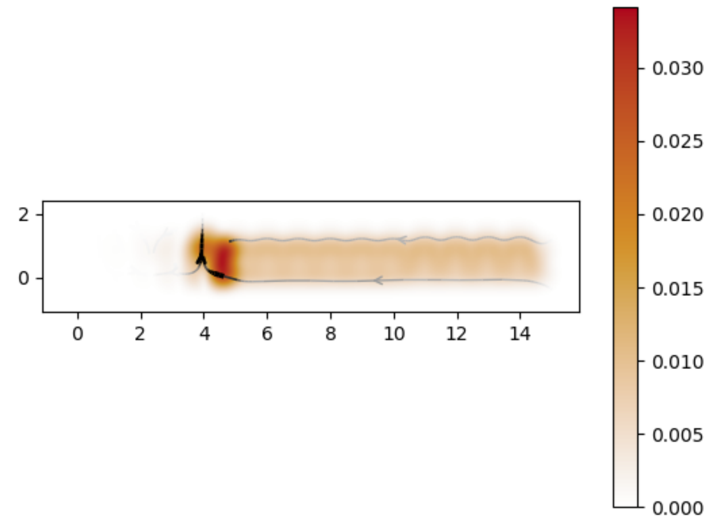

spin current – y component

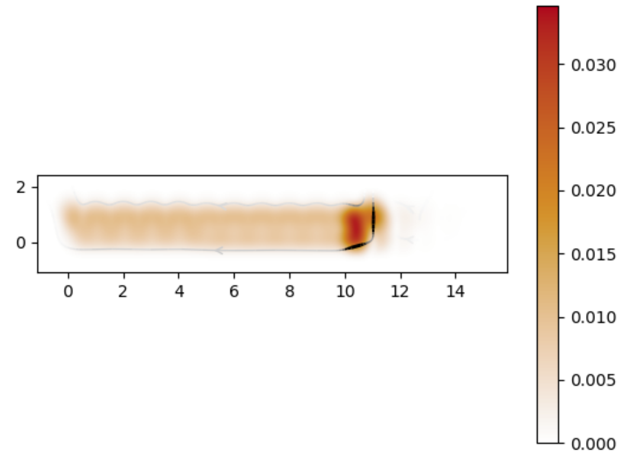

spin current – x component

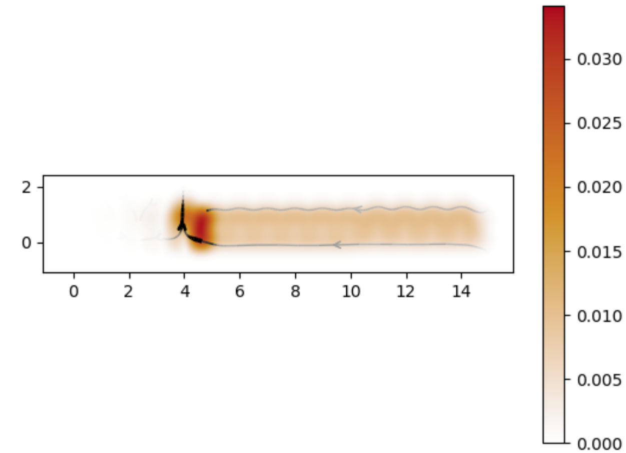

spin current – y component

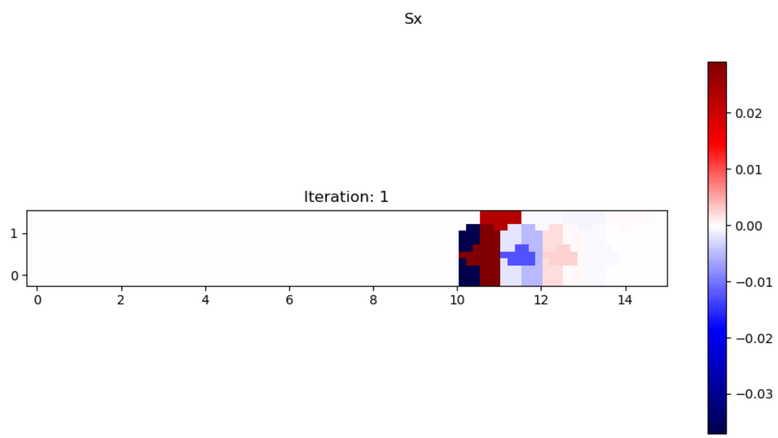

Spin x source

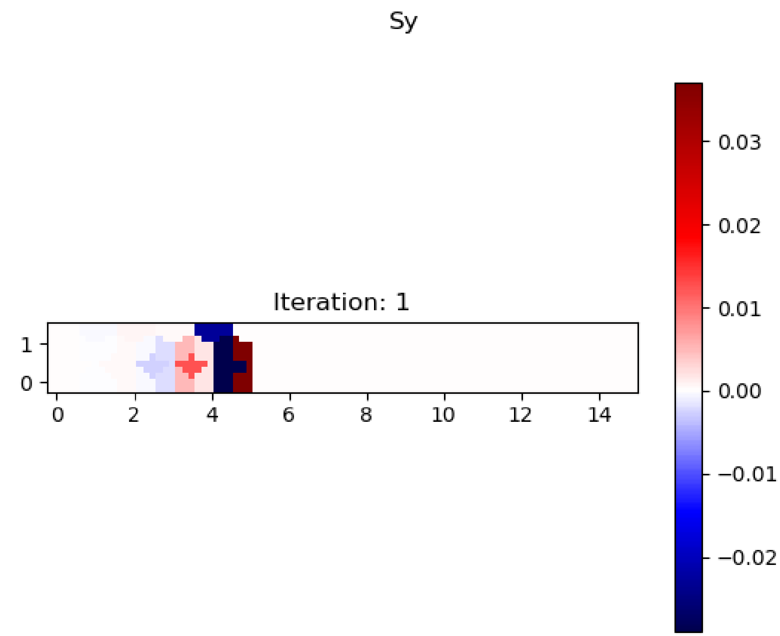

Spin y source

Magnetic random access memories

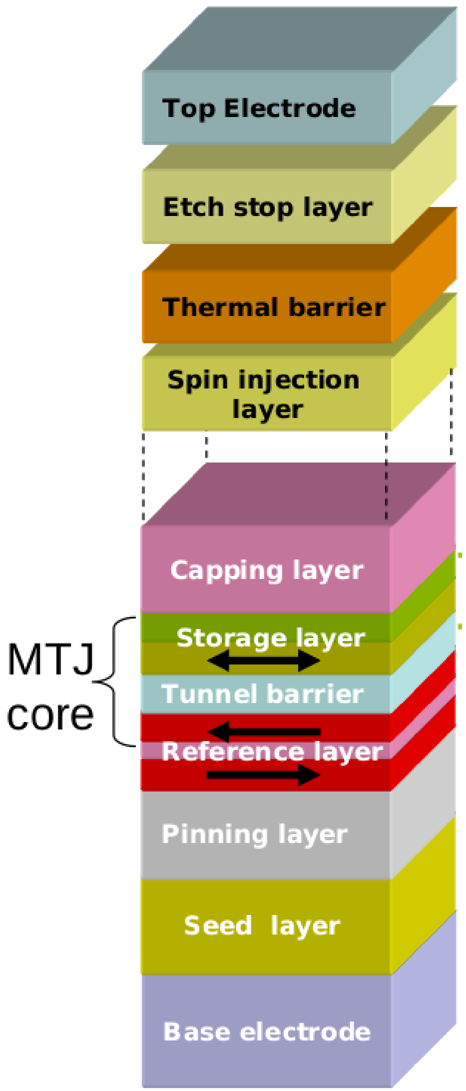

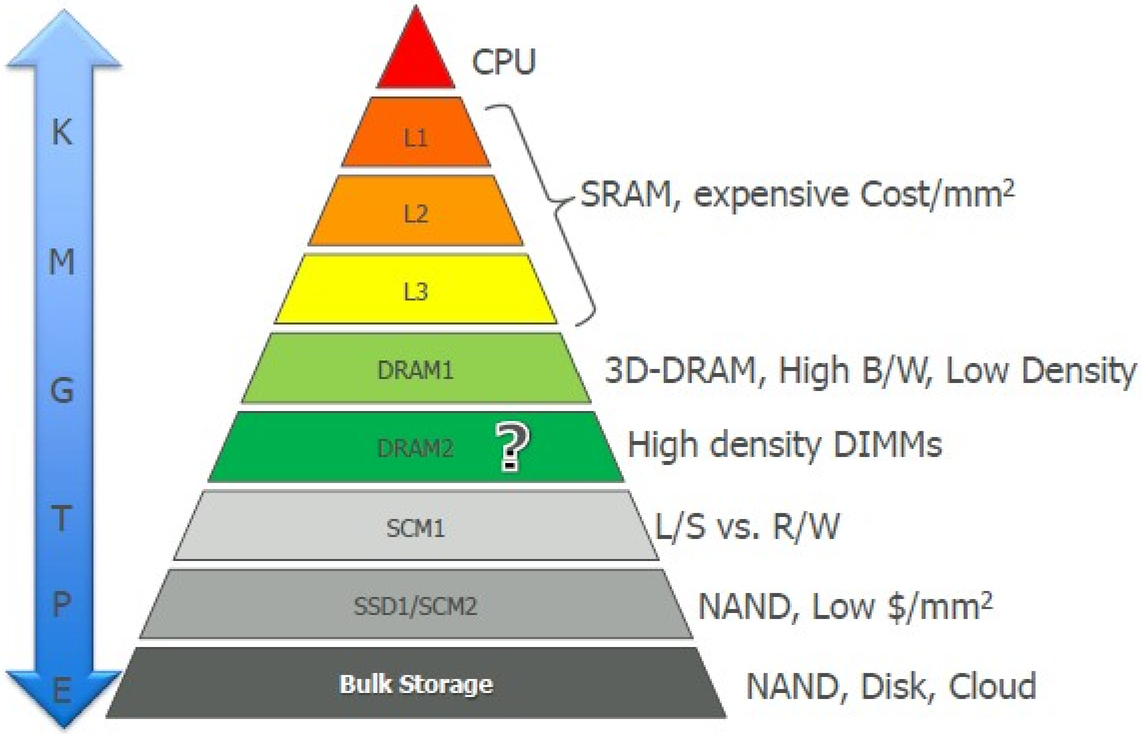

MRAMs are expected to be on the market soon

Bulk systems

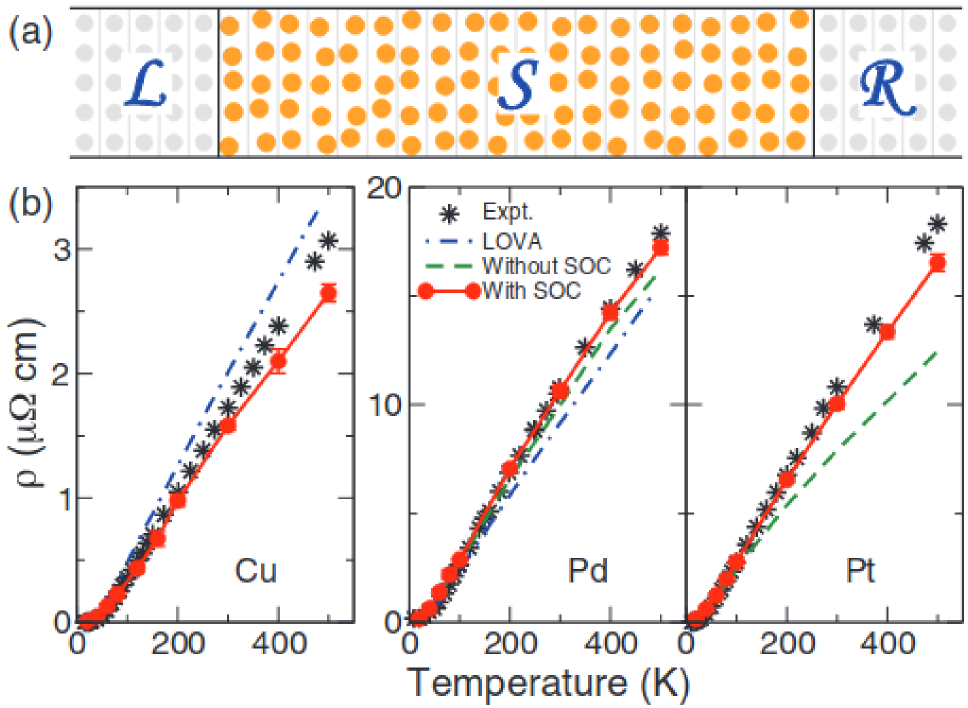

FIG. 1. (Color online) (a) Illustration of the scattering geometry used to calculate transport properties. By populating first-principles phonon modes, we generate correlated lattice disorder in a scattering region ($\mathcal{S}$) that is connected to semi-infinite, crystalline left ($\mathcal{L}$) and right ($\mathcal{R}$) leads. (b) Temperature-dependent electrical resistivities calculated for Cu, Pd, and Pt. The green dashed lines for Pd and Pt are results obtained without SOC. Experimental data (black stars) [15,16] and the results of LOVA calculations (blue dashed-dotted lines) [3] are shown for comparison.

Phys. Rev. B 91, 220405(R) (2015)

Bulk systems

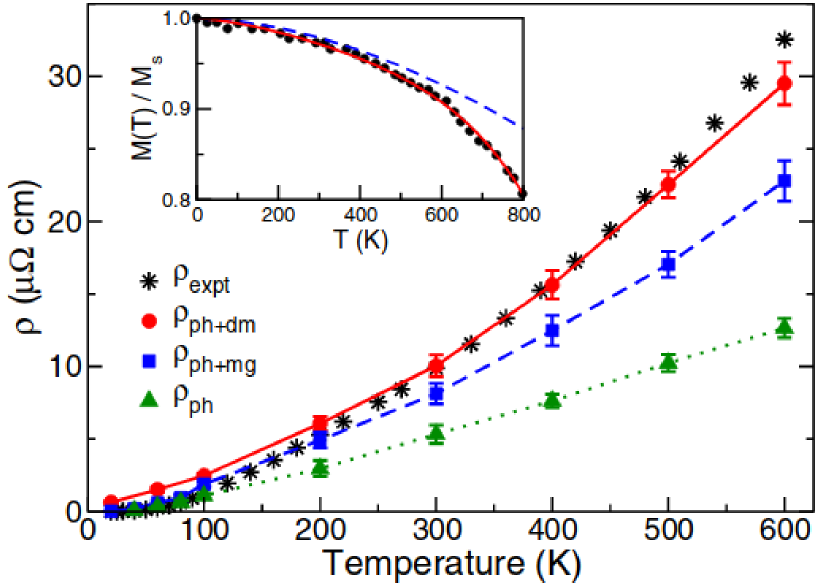

FIG. 3. (Color online) Electrical resistivity for bcc Fe calculated as a function of the temperature. Green triangles: Resistivity arising from phonon-induced lattice disorder. Blue squares: Resistivity in the presence of phonons and magnons that are both populated in the scattering region at a given temperature. Red circles: Resistivity with phonon lattice disorder and uncorrelated spin disorder that reproduces the experimental demagnetization curve (inset). The experimental values [16] are plotted as black stars for comparison. Because of the smallness of the anisotropic magnetoresistance in Fe [32,33], we only consider the case of magnetization parallel to the current direction. Inset: Temperature-dependent magnetization of Fe from experiment (black dots) [34] and obtained by populating magnons (blue dashed line). The red line interpolates the experimental values using a cubic spline method.

Phys. Rev. B 91, 220405(R) (2015)